

# CIVA

J.-P. BIBRING<sup>1,\*</sup>, P. LAMY<sup>2</sup>, Y. LANGEVIN<sup>1</sup>, A. SOUFFLOT<sup>1</sup>, M. BERTHÉ<sup>1</sup>,  
J. BORG<sup>1</sup>, F. POULET<sup>1</sup> and S. MOTTOLA<sup>3</sup>

<sup>1</sup>*IAS, Institut d'Astrophysique Spatiale, Orsay, France*

<sup>2</sup>*LAM, Laboratoire d'Astrophysique de Marseille, Marseille, France*

<sup>3</sup>*IWP/DLR, Berlin*

(\*Author for correspondence: E-mail: bibring@ias.fr)

(Received 26 June 2006; Accepted in final form 28 November 2006)

**Abstract.** CIVA (Comet Infrared and Visible Analyser) is an integrated set of imaging instruments, designed to characterize the 360° panorama (CIVA-P) as seen from the Rosetta Lander Philae, and to study surface and subsurface samples (CIVA-M). CIVA-P is a panoramic stereo camera, while CIVA-M is an optical microscope coupled to a near infrared microscopic hyperspectral imager. CIVA shares a common Imaging Main Electronics (IME) with ROLIS. CIVA-P will characterize the landing site, with an angular sampling (IFOV) of 1.1 mrad: each pixel will image a 1 mm size feature at the distance of the landing legs, and a few metres at the local horizon. The panorama will be mapped by 6 identical miniaturized micro-cameras covering contiguous FOV, with their optical axis 60° apart. Stereoscopic capability will be provided by an additional micro-camera, identical to and co-aligned with one of the panoramic micro-camera, with its optical axis displaced by 10 cm. CIVA-M combines two ultra-compact and miniaturised microscopes, one operating in the visible and one constituting an IR hyperspectral imaging spectrometer: they will characterize, by non-destructive analyses, the texture, the albedo, the molecular and the mineralogical composition of each of the samples provided by the Sample Drill and Distribution (SD2) system. For the optical microscope, the spatial sampling is 7  $\mu\text{m}$ ; for the IR, the spectral range (1–4  $\mu\text{m}$ ) and the spectral sampling (5 nm) have been chosen to allow identification of most minerals, ices and organics, on each pixel, 40  $\mu\text{m}$  in size. After being studied by CIVA, the sample could be analysed by a subsequent experiment (PTOLEMY and/or COSAC). The process would be repeated for each sample obtained at different depths and/or locations.

**Keywords:** cometary composition, in situ imaging, microscopic analyses

## 1. Scientific Rationale

The origin and history of a comet is recorded both in microscopic and macroscopic properties of its surface: sizes, shapes, molecular and mineralogical composition of constituent materials, from micron-sized individual grains and matrix components, up to meter size or larger crust features and boulders. The combined imaging of the Rosetta Lander landing site, up to the horizon, and analyses of surface and subsurface (drilled) samples can reveal unique information about the composition of the primordial molecular protosolar cloud, the initial states of formation of planetesimals in the solar nebula and their subsequent processing. This record of the physical and chemical processes of aggregation, accretion and evolution is

unique. It will provide key information on which and how molecules, condensates and grains form during the collapse of the protosolar molecular cloud, up to the present planetary system (Irvine and Lunine, 2004).

### 1.1. SOLAR NEBULA ACCRETION PROCESSES

Cometary nuclei are the icy planetesimals of the outer Solar System. They were likely the first bodies to form in the solar nebula and the building blocks of the giant planets core and satellites. As such, comets record the physical processes that brought grains of ice, silicates and organics together in the solar nebula (Weidenschilling, 2004). Did the organics and/or ices cement grains together? Was the accretion process accomplished through the gentle settling of grains to the nebula midplane, or did it involve more violent collisions in turbulent eddies in the collapsing nebula? Were chondrules incorporated into the forming comet? How was material subsequently modified during the comets long storage in the Oort cloud and Kuiper belt? Such questions can be addressed by studying cometary samples and the cometary surface at the relevant sizes and length scales.

### 1.2. COMETARY PROCESSING

A wide variety of processes have been identified which could alter cometary nuclei, in particular their near-surface layers, prior to and during their evolution through the inner Solar System, as active comets. These include irradiation by early and/or present solar wind particles, solar and galactic cosmic rays, impacts by cometary and asteroidal debris, and solar heating. The combined effects of these various processes, as for example amorphous-to-crystalline ice phase transitions, irradiation-induced molecular synthesis, development of a nonvolatile crust, steady and transient outgasings, will be studied in depth by in situ imaging and spectroscopic investigations. It then might be possible to answer questions such as: at what scale (microscopic or macroscopic?) does surface heterogeneity (ice/crust) appear? What are the sizes of the features associated to the outgassing processes? Is the original irradiated crust retained, and serves as a basis for further crust development, or is this primitive irradiated crust blown off by cometary gas pressure as the nucleus approaches the Sun, to be replaced by a latter deposit of large, nonvolatile grains? How deep do the processed layers extend and what is their physical nature and composition as a function of depth? Is the crust material porous, allowing the free passage of evolved gases, or does it become clogged with cometary particulates? How close to the nucleus surface does one find volatile ices? In what form are the volatiles: molecular ices, clathrates, adsorbates, solutions? Were near-surface crust materials modified by processes similar to those seen in meteorites, such as aqueous alteration (Hanner and Bradley, 2004)? Are cometary surface materials present in terrestrial meteorite collections? This latter question has the potential

of generating new direction in meteoritics and studies of early Solar System chemistry.

### 1.3. PRIMORDIAL CHEMICAL EVOLUTION

Although the ground observation of interstellar clouds demonstrates that an efficient chemistry takes place as the density increases during their collapse, we cannot probe directly clouds with densities high enough to enable protoplanetesimals to form. The comets are unique bodies recording the final molecular state of a protostellar cloud – and in particular that of the protosolar nebula. Their study should provide the answer to a key question, with implications for the further chemical and biological evolution within the Solar System: to which level of chemical complexity did this cloud evolve? Halley flybys in 1986 strongly indicated the existence of refractory organics as constituents of cometary nuclei (Combes *et al.*, 1986; Kissel *et al.*, 1987), without being able to identify them precisely. It is one of the major goals of the Rosetta mission as a whole, and of our investigation, to achieve this identification. The importance is based on the possibility that comets, impacting on planetary surfaces, did feed early oceans with complex molecules, playing an important role in (bio)chemical evolution.

### 1.4. SPECTRAL PROPERTIES OF CANDIDATE COMETARY MATERIALS

Our goal is to contribute to unambiguously identify the volatiles (the parent molecule reservoir) as well as the refractory minerals and organic compounds of the collected samples. Infrared reflectance spectroscopy is a well-developed and powerful technique used to determine molecular and mineralogical composition. It is an especially potent method when high spatial and spectral resolution are combined, giving pure signatures of individual grains in an inhomogenous sample. CIVA-M uses a spectral range which is rich in sharp, diagnostic spectral features that can be used to determine the abundance of the chemicals comprising the grains and matrix material of the comet samples. The position and shape of these features are also indicative of the physical state of the existent molecules.

Parent molecules such as H<sub>2</sub>O, NH<sub>3</sub>, NH<sub>4</sub>SH<sub>3</sub>, H<sub>2</sub>CO, CH<sub>3</sub>OH, CH<sub>3</sub>CN, HCN, H<sub>2</sub>S, CO, CO<sub>2</sub> and CH<sub>4</sub> can be identified in the spectral range 1 to 4 μm. The spectral signatures are generally sharp, and their shapes and positions can be accurately determined using the high spectral resolution of CIVA-M, giving information on the physical state of the minerals. The high performances of CIVA-M allow the determination of trace molecules at the fraction of a percent level, as well as some isotopic determinations. The present observations of the surface of Mars by an infrared spectral imager (OMEGA) operating in the same wavelength range on board the Mars Express mission (Bibring *et al.*, 2004a) demonstrates the potential of near infrared reflectance spectrometry as a diagnostic tool: H<sub>2</sub>O and CO<sub>2</sub> ices are readily

detectable (Bibring *et al.*, 2004b; Langevin *et al.*, 2006); the iron-containing silicates such as olivine and pyroxene can be identified through their well-characterized  $\sim 1 \mu\text{m}$  and  $\sim 2 \mu\text{m}$  bands (Mustard *et al.*, 2005); hydrated minerals can be identified through the  $\sim 1.9 \mu\text{m}$  and  $\sim 3.0 \mu\text{m}$  water-of-hydration band, and discriminated through their metal-OH transitions, between 2 and  $2.4 \mu\text{m}$  (Poulet *et al.*, 2005).

The organic “CHON” material, likely to be similar to the one identified by IKS/VEGA through its  $3.3\text{--}3.5 \mu\text{m}$  feature, can be classified through functional group analysis, using the positions and intensities of the  $-\text{CH}_2$  and  $-\text{CH}_3$  groups, and the aromatic group adsorptions. Ground-based measurements of “CHON” material in cometary comae, as well as our own laboratory work on refractory organic analogues, show that a spectral resolving power greater than 300 is necessary and adequate to characterize the material.

Modern computational techniques, and a growing library of optical data for simple and complex molecules (and their various mixtures) enable quantitative spectral modelling to determine not only the identity and relative abundances of the constituents, but important information on the physical state of the molecular mixtures of these constituents.

### 1.5. CIVA INVESTIGATIONS

On board Philae, CIVA will investigate these questions of early chemical evolution, cometary formation and processing. This will be accomplished by stereoscopic imaging of the site surrounding the Lander (CIVA-P), and by optical imaging and infrared spectral imaging of surface and subsurface samples of the cometary nucleus, at a microscopic scale (CIVA-M).

CIVA will analyse cometary material from micron size particles to meter size features:  $7 \mu\text{m}$  to a few mm with the microscope, 1 mm to meters with the panoramic cameras. Grains with size smaller than 1 cm are likely to represent the major fraction of the non volatile mass of the nucleus, which constitutes predominantly the meteoroid streams, the interplanetary dust particles and the micrometeorites, for which CIVA results will serve as ground truth. Study of pristine and processed nucleus materials in this size range will greatly improve our understanding of what are and how matured are cometary ices, minerals and organics.

The CIVA investigations are intimately related to others on board Rosetta. To a large extent, CIVA will provide ground truth data for a number of remote sensing imaging and spectral investigations performed from the Orbiter: it will complement, at a higher resolution but on a restricted (landing) site, the global mapping OSIRIS will provide. The IR spectral imaging at microscopic sample level will be efficiently compared to the global meter-scale hyperspectral mapping VIRTIS will obtain, in the same near infrared domain. The microscopic and spectral sample analyses will complement MIDAS, GIADA and COSIMA data. On the Lander,

MUPUS, ROMAP and SESAME will use the panoramic images to view and/or locate their sensors after deployment, and characterize their context with respect to the local environment. The CIVA-M non-destructive microscopic imaging and IR molecular spectrometry will precede PTOLEMY and/or COSAC studies: the same samples will then be processed, through stepwise heatings, by chemistry and/or gas chromatography, to isolate species then analysed by mass spectrometry. This combined protocol, similar to the one followed in terrestrial laboratories, has the potential of unambiguously identifying cometary constituents, including refractory organics.

## 2. CIVA-P

The panoramic camera will characterize the surface topography and provide an albedo mapping of the landing site, with the aim of describing the interfaces between dark mantle materials and brighter surface ices at all scales; it will identify structures (microcracks, vents, faults) and erosion features linked to cometary processes; it will reconstruct the local 3-dimension structure of the surface, in at least one  $60^\circ$  FOV including a landing leg, the penetration of which will indicate the tensile strength of the cometary material. With the rotation of Philae, the stereoscopic reconstruction can be obtained for the full panorama. In addition, if operations of CIVA-P are repeated several times along the cometary activity, surface changes, resulting for example from microjets, and faint dust emissions will be detected at scales not achievable from the Orbiter.

CIVA-P consists of 7 identical miniaturized cameras, implemented as 5 single cameras and one stereoscopic pair of two co-aligned ones, thus filling the  $360^\circ$  panoramic field of view by six contiguous FOV of  $60^\circ$  each,  $60^\circ$  apart one from the next (Figure 1). The spectral response of each camera, integrating the properties of both the detector and the optics, extends from 400 to 1100 nm, with a transmission higher than 50% from 550 nm to 850 nm, and a maximum around 700 nm.

The camera heads are integrated into 3D miniaturized cubes (Figures 2 and 3, Table 1), on top of which the detector is located: it is a frame transfer  $1024 \times 1024$  pixels CCD. The cube ( $70 \times 52 \times 36 \text{ mm}^3$ , including the optics, as in Figure 2) includes all driving electronics, with its FPGA based controller. The development of these pioneering highly integrated microcameras, supported by CNES, was led by IAS (Orsay) in collaboration with LAM (Marseille), and conducted in partnership with a selected industrial consortium, led by CSEM, with TCS (Atmel) and 3D+. The cameras have been qualified at low temperatures both for storage (120 K) and operation (170 K).

All cameras are mounted at the top of the side panels of the Lander. For the five panels covered with solar cells, cells have been removed to give clearance for the camera FOV (Figure 4). The single and stereo cameras are tilted down by  $15^\circ$

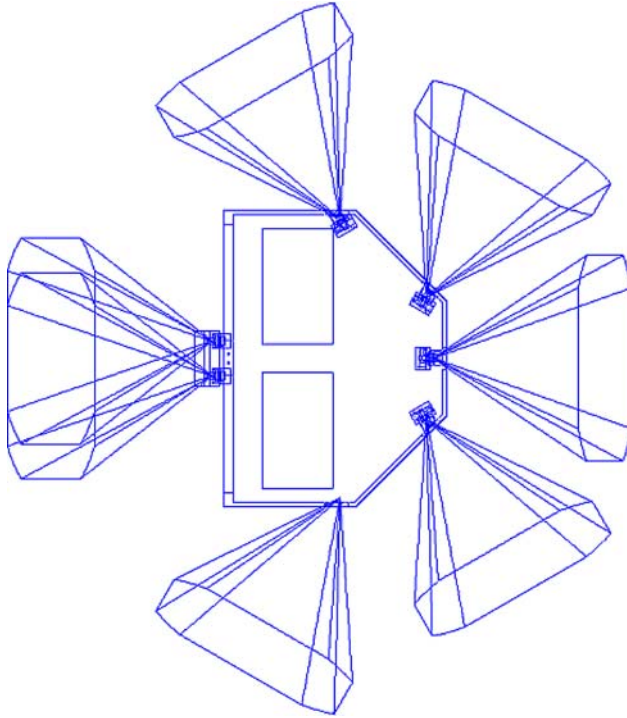


Figure 1. Philae top view, with the location of the 7 CIVA-P cameras and the sketch of their FOV.

and  $25^\circ$  from the “horizontal” plane (Philae baseplate) respectively. The mass of CIVA-P (5 panoramic monocameras and one pair of stereocameras) is 1190 g plus 460 g for its electrical harness.

The seven cameras are operated sequentially. The electronics driving each CCD has adequate intelligence to autonomously optimise the exposure time. All images are compressed by the CIVA-CDPU, and stored (in the IME) before being transmitted.

### 3. CIVA-M

CIVA-M is constituted of a visible microscope, CIVA-M/V and a near infrared hyperspectral imager CIVA-M/I. CIVA-M/V (Figure 5) and CIVA-M/I (Figure 6) are mounted on the Philae base-plate (“balcony”), close to the drill and sample distribution system (SD2). They will image and analyse the samples (from a distance of 13.0 mm) whenever they will be deposited within containers (“Mid Temperature Ovens”), mounted on a rotating carousel, and closed by a sapphire window transparent in both the Visible and the near IR (Table 2).

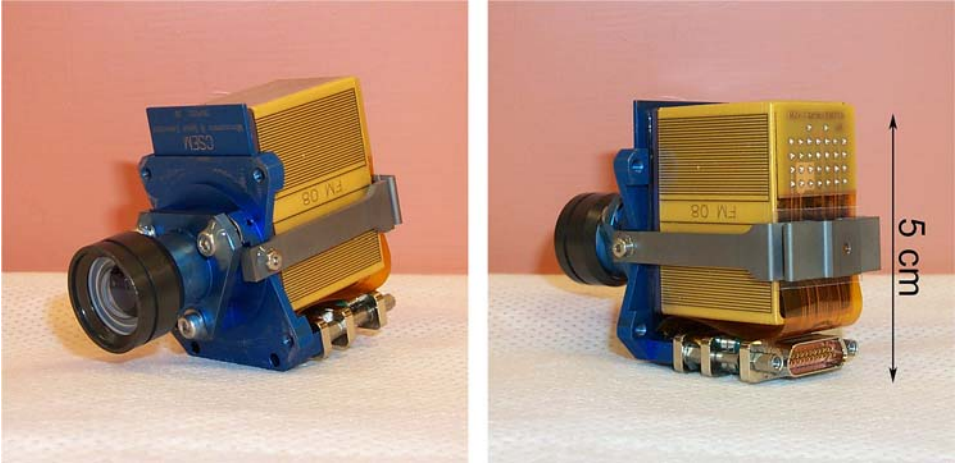


Figure 2. One CIVA-P FM camera before implementation on Philae.

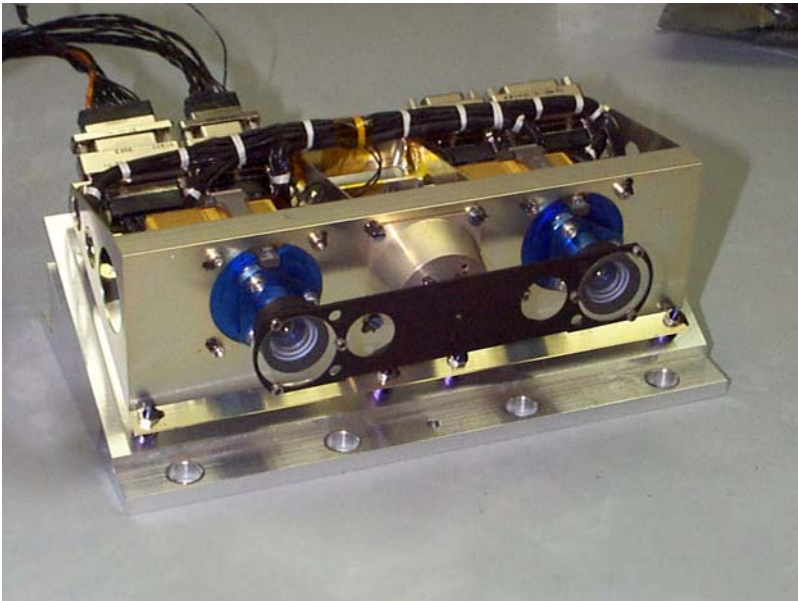


Figure 3. The CIVA-P stereo camera.

Both CIVA-M/V and CIVA-M/I have their own source to illuminate the samples, enabling operations to be performed at night. Daytime operations are also feasible, since the actual opto-mechanical interface between CIVA-M and the ovens strongly minimizes the potential for straylight radiation to reach the sample.

CIVA-M/V will image the samples onto a  $1024 \times 1024$  CCD detector (3D cube identical to the ones used for CIVA-P), with a spatial sampling of

TABLE I  
CIVA-P characteristics and performances.

Number of heads	5 (Single) + 2 (Stereo)	Integration time (typical)	0.2 s
Mean IFOV	1.02 mrad (3.5 arcmin)	Duration of imaging cycle (typical)	≈80s
FOV	1.05 rad (60°)	N° of images	7
Spectral response	Maximum @ 700 nm	SNR	> 100
Spectral sampling	n/a	Dynamic range	10 bits
Spatial sampling	1 mm/pix @ 1 m	Data volume (compressed typical)	1.2 Mbit per image
Stereo imaging	Yes	Single Total Mass (g)	140
Artificial illumination	No	Stereo Total Mass (g)	490
Illumination optics	n/a	Total Mass (g) (without harness)	1190
Focal ratio	f/10	Camera size (w/o optics)	46 × 52 × 36 mm <sup>3</sup>
		Camera size (w optics: Figure 2)	70 × 52 × 36 mm <sup>3</sup> (single)
		Camera size (stereo: Figure 3)	112 × 195 × 90 mm <sup>3</sup> (stereo)
Detector	1024 × 1024 CCD	Power consumption (W) (heater not included)	~1.5 per camera head
Storage temperature	≥ 120 K	Mounting position	Top inner side panels
Operating temperature	≥ 170 K	Measurement period	Day



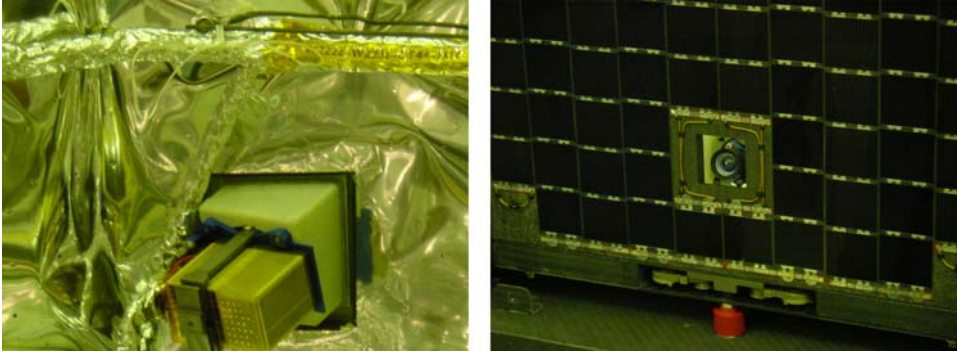


Figure 4. Close-up of one CIVA-P flight camera (inside view, left; outside view, right).



Figure 5. CIVA-M/V FM, prior to implementation on Philae.

$7\ \mu\text{m}$  and a large depth of focus (up to  $\pm 0.1\ \text{mm}$ ); the samples will be illuminated sequentially with 3 LEDs, at  $525\ \text{nm}$  (green/blue),  $640\ \text{nm}$  (red) and  $880\ \text{nm}$  (near IR). Its mass is  $276\ \text{g}$ , and its size  $70 \times 50 \times 94\ \text{mm}^3$  (footpads excluded).

Following the microscope imaging, IR spectral images will be obtained, with a spatial sampling of  $40\ \mu\text{m}$ , onto a  $128 \times 128$  photovoltaic HgCdTe array operating at temperatures  $120$  to  $140\ \text{K}$ , provided by a passive (radiator) cooling. CIVA-M/I will give an image of each sample and the spectrum of every pixel of this image,  $40\ \mu\text{m}$  in size, to infer the molecular and mineralogical composition. More precisely, CIVA-M/I includes a white source ahead of a grating monochromator that will be operated



Figure 6. CIVA-M/I FM, prior to implementation on Philae.

in the following way. The sample will be illuminated by a monochromatic light that can be scanned over the spectral range 1 and 4  $\mu\text{m}$  by steps of 3 nm using the rotation of the grating (the resolving power varies from 100@ 1  $\mu\text{m}$  to 600@ 4  $\mu\text{m}$ ). At each step, a monochromatic image will be taken. Thus, a total of about 750 images will be acquired sequentially, each at a different wavelength, leading to a 3-dimensional (two spatial and one spectral) “image-cube”. The range and resolution have been chosen to allow identifying not only the major minerals, but also the icy volatiles and the major chemical functions of organic refractories. The entire process will take less than 20 min, to get all spectra with SNR >100, assuming IR albedos of 0.05. The mass and size of CIVA-M/I are: 455 g and 80  $\times$  50  $\times$  120 mm<sup>3</sup>.

For both CIVA-M/V and CIVA-M/I, the operational procedure includes the imaging of a calibration target, constituted of a reference material (Al<sub>2</sub>O<sub>3</sub>) implemented in one of the oven. These in-flight calibrations, repeating those performed on the ground and during cruise, will be used to monitor the potential aging of the units. In addition, it is foreseen to image each oven prior to their filling with cometary samples, so as to discriminate the specific cometary features from potential contaminants.

As for CIVA-P, all data will be processed by the CIVA-CDPU before being stored and transferred to the CDMS for their further downlink.

#### 4. CIVA-Electronics

The Imaging Main Electronics (IME) is a facility, developed under the co-responsibility of IWP/DLR and IAS, for both ROLIS and CIVA: they share a

TABLE II  
CIVA-M characteristics and performances.

Channel	Microscope (M/V)	IR spectrometer (M/I)
Number of heads	1	1
IFOV	$7\ \mu\text{m} \times 7\ \mu\text{m}$	$40\ \mu\text{m} \times 40\ \mu\text{m}$
FOV	3 mm diameter	3 mm diameter
Wavelength range	525 nm, 640 nm, 880 nm	1–4 $\mu\text{m}$
Spectral sampling	3 LEDs, 20 nm each	10 nm at 4 $\mu\text{m}$
Spatial sampling	7 $\mu\text{m}/\text{pix}$	40 $\mu\text{m}/\text{pix}$
Stereo imaging	No	No
Artificial illumination	LEDs	Monochromator
Illumination optics	n/a	Same as foreoptics
Focal ratio	f/20	f/3.5
Detector	1024 $\times$ 1024 CCD	128 $\times$ 128 HgCdTe
Operating temperature		
Detector	$\geq 170\ \text{K}$	120–140 K
Optics		150–200 K
Integration time (typ.)	0.01–1 s	$< 1\ \text{s}/\Delta\lambda$
Duration of measurement cycle (typ.)	60 s	$< 1000\ \text{s}$
No. of cycles (one per sample)	10	10
S/N	$> 100$	$> 100$
Dynamic range	10 bits	12 bits
Data volume (compressed)	5 Mbit/sample	$\sim 24\ \text{Mbits}$ /spectrum.sample
Mass (g)	276	455
Box envelope (footpads and radiator not included)	$70 \times 50 \times 94\ \text{mm}^3$	$80 \times 50 \times 120\ \text{mm}^3$
Radiator size		$90 \times 160\ \text{mm}^2$
Power consumption (W)	$\sim 2.2$ (heater included)	$\sim 8.4$
Mounting position	Philae baseplate (balcony)	
Measurement period	Favoured at night	

common interface with the Lander, for both the power subsystem and the Central Data Management System (CDMS). The IME includes the CIVA-Central Electronics (CIVA-CE), mainly based on a dedicated CDPU (Command and Data Processing Unit); it is equipped with a 16 Mbytes mass memory.

The CIVA-CDPU (Command and Data Processing Unit), developed by IAS, has the following functions: on/off power control; camera program uploading; camera heads check-out; command reception (from ROLIS-DPU) and management; CIVA payload sequencing; status monitoring; image acquisition; integration time

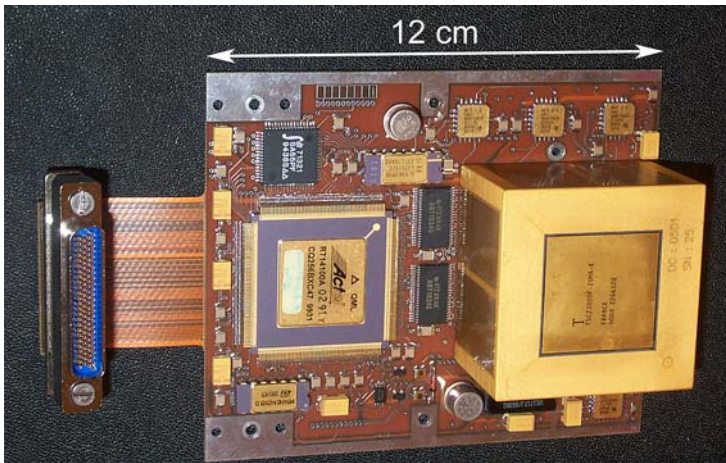


Figure 7. CIVA-CDPU integrated on its board.

optimisation; image compression (using wavelet based software); error encoding and data formatting.

It consists of a TEMIC TSC21020 processor, 2 Kwords PROMs for boot sequence, 512 Kbytes EEPROM for application program and parameters storage, 128 Kwords Fast SRAM for application program, 128 Kwords Fast SRAM for application data and 6 Mbytes SRAM for 2 images data ( $1024 \times 1024$  pixels) storage/processing. The CDPU electronics is integrated into a 3D-packaged cube which is implemented into the IME (Figure 7).

The CIVA-CE includes two more electrical boards: one is dedicated to the IR detector, and the second to the CIVA peripherals.

## 5. Scientific Sequences

CIVA-P will be operated to take one stereo image of the Orbiter just after release of Philae, to be used as calibration for the on-comet images. Then, immediately after touch-down, a full panorama of the landing site, with a partial stereoscopic coverage, will be taken by CIVA-P, and immediately transmitted to the Earth for quick look data reduction. This first panorama will be key to assess the landing conditions, and to declare secure the planned Philae sequence of operations. Follow-on partial or global panoramas could be acquired either to monitor changes with solar illumination and/or cometary activity, to increase the stereoscopic coverage, and to image after their deployment Philae systems and sensors.

CIVA-M will be turned on after all samplings (surface and subsurface) by SD2. It will consist in sequences of calibration (by imaging an oven with a calibration target), imaging of ovens prior to be filled, and after being filled by SD2 with

cometary samples. CIVA-M/V will image each oven in three colors, while CIVA-M/I will acquire a complete 3D ( $x, y, \lambda$ ) image-cube of them. After compression and storage in the IME mass memory, the data will be transferred to CDMS for downlink.

## 6. In Flight Calibrations

During the cruise, a number of active calibrations have been and still will be performed, demonstrating the full functionality of all systems. However, as it is facing the Orbiter, the balcony has an equilibrium radiative temperature of  $\sim 160\text{K}$ , which is still too high for the IR detectors to operate: until Philae will be ejected from the Orbiter, all CIVA-M/I images will remain saturated. This is not the case for the optical CCD-based systems. CIVA-M/V has already acquired three-color images of both the calibration target (Figure 8, left) and of an empty oven (Figure 8, right). The enlargement (Figure 9) shows that the image quality achieved in flight is strictly consistent with the goal ( $\sim 7 \mu\text{m}$  spatial sampling).

Similarly, CIVA-P has already acquired spectacular images of the rear side of the Orbiter solar panels (Figure 10). With different integration times, CIVA-P detects

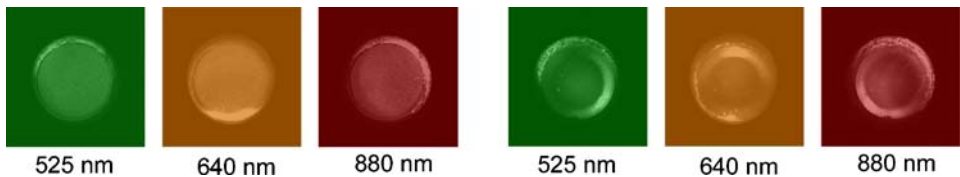


Figure 8. CIVA-M 3-color in-flight imaging of the calibration (left) and an empty (right) oven.

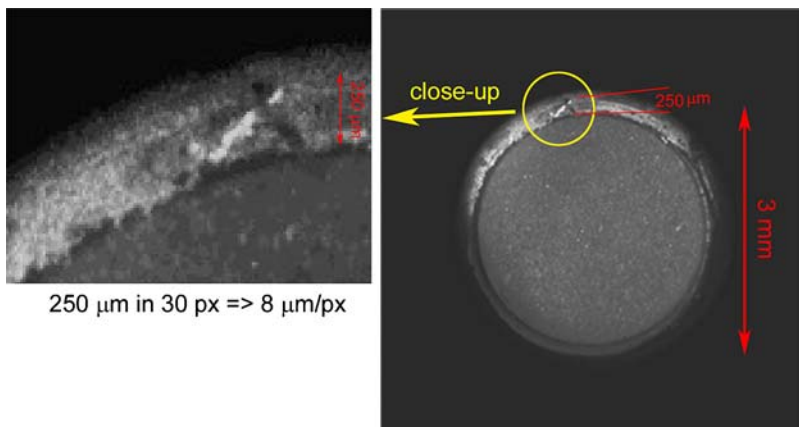


Figure 9. Enlargement of a CIVA-M in-flight oven imaging, indicating the spatial sampling.



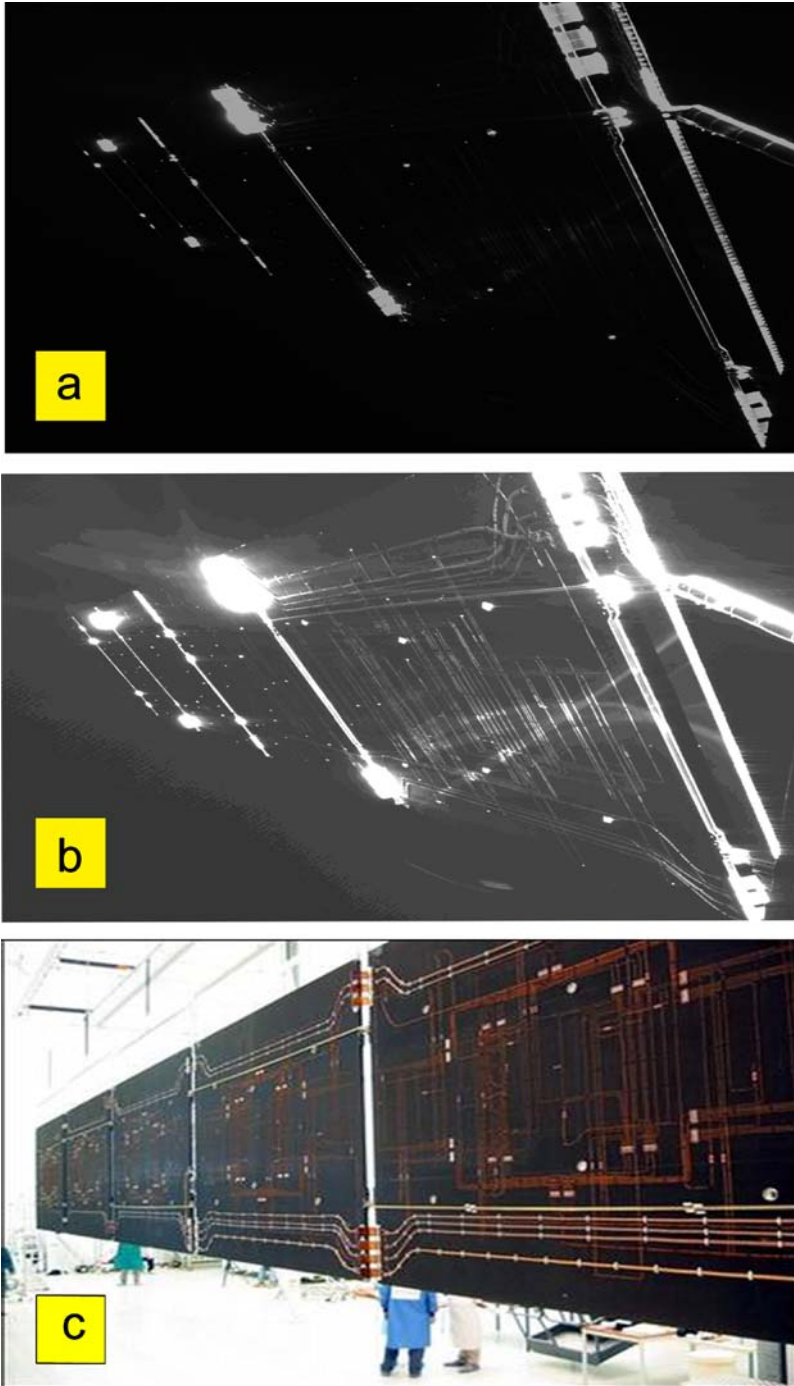


Figure 10. CIVA-P in-flight imaging of one solar panel with (a) low exposure time, and (b) enhanced exposure time, compared to a corresponding ground picture (c).

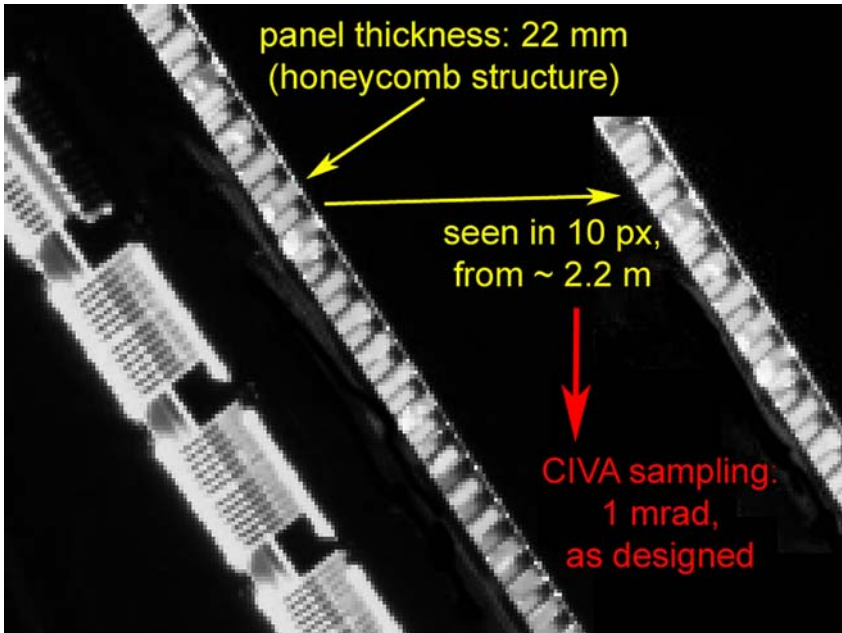


Figure 11. Enlargement of Figure 10a, enhancing the CIVA-P resolution achieved in imaging the solar panel honeycomb structure.

very faint structures, although they were in full shadow, only illuminated by stray light reflections. The enlargement (Figure 11) exhibits the full consistency of the achieved spatial sampling with its goal.

## References

- Bibring, J.-P., Soufflot, A., Berthé, M., Langevin, Y., Gondet, B., Drossart, P., *et al.*: 2004a, *ESA SP* **1240**, 37.
- Bibring, J.-P., Langevin, Y., Poulet, F., Gendrin, A., Gondet, B., Berthé, M., *et al.*: 2004b, *Nature* **428**, 627.
- Combes, M., Moroz V. I., Crifo, J. F., Lamarre, J. M., Charra J., Sanko N. F., *et al.*: 1986, *Nature* **321**, 266.
- Hanner, M. S., and Bradley, J. P.: 2004, in M. Festou, H. Keller, and H. Weaver (eds.), *Comets II*, University of Arizona Press, Tucson, p. 555.
- Irvine, W. M., and Lunine, J. I.: 2004, in M. Festou, H. Keller, and H. Weaver (eds.), *Comets II*, University of Arizona Press, Tucson, p. 25.
- Kissel, J., and Krueger, F. J.: 1987, *Nature* **326**, 755.
- Langevin, Y., Douté, S., Vincendon, M., Poulet, F., Bibring, J.-P., Gondet, B., *et al.*: 2006, *Nature* **442**, 790.
- Mustard, J. F., Poulet, F., Gendrin, A., Bibring, J.-P., Langevin, Y., Gondet, B., *et al.*: 2005, *Science* **307**, 1594.

- Poulet, F., Bibring, J.-P., Mustard, J. F., Gendrin, A., Mangold, N., Langevin, Y., *et al.*: 2005, *Nature* **438**, 623.
- Weidenschilling, S. J.: 2004, in M. Festou, H. Keller, and H. Weaver (eds.), *Comets II*, University of Arizona Press, Tucson, p. 97.